Latent Fingerprint Matching

Anil K. Jain, Abhishek Nagar and Karthik Nandakumar

Abstract

Latent fingerprint identification is of critical importance in forensics. While tremendous progress has been made in the field of automatic fingerprint identification, latent fingerprint matching continues to be a difficult problem because the challenges involved in latent print matching are quite different from rolled (full) fingerprint matching. Poor quality of friction ridge impressions, small finger area and large non-linear distortion are the main factors that affect latent fingerprint matchers. We propose a system for matching latent images with full fingerprints that uses minutiae as well as ridge information as the discriminative features. We have developed a minutiae-based fingerprint matcher that takes into account the specific characteristics of the latent matching problem. The ridge correlation matcher determines the degree of similarity in the ridge flow patterns of latents and full-print images. Experimental results on the NIST Special Database-27 which consists of 258 latents and their corresponding full fingerprint images indicate that the fusion of minutiae and ridge correlation matchers leads to good recognition performance despite the inherently difficult nature of the problem.

Index Terms

Latent fingerprints, fingerprint matching, minutiae matcher, ridge-correlation.

This research was supported by the National Institute of Justice.

I. INTRODUCTION

Fingerprint images can be broadly classified into three categories, namely, (i) rolled/full, (ii) plain/flat and (iii) latent [1]–[3] (see Figure 1). Rolled fingerprint images are obtained by rolling a finger from one side to the other ("nail-to-nail") in order to capture all the ridge-details of a finger. Plain impressions are those in which the finger is pressed down on a flat surface but not rolled. While plain impressions cover a smaller area than rolled prints, they typically do not have the distortion introduced during rolling. Rolled and plain impressions are obtained either by scanning the inked impression on paper or by using live-scan devices. Since rolled and plain fingerprints are acquired from co-operative subjects, they are typically of high quality and rich in information content. In contrast, latent fingerprints are lifted from surfaces of objects that are inadvertently touched or handled by a person through a variety of means ranging from simply photographing the print to more complex dusting or chemical processes [4], [5]. It is the latent fingerprints that are of utmost importance in forensics to apprehend a criminal or to verify the identity of a suspect.

(a) (b) (c)

Fig. 1. Three types of fingerprint images. (a) Rolled/full print, (b) Plain/flat print and (c) Latent print.

Latent fingerprints obtained from crime scenes have served as crucial evidence in forensic identification for more than a century. However, there have been instances where mistakes in latent fingerprint identification have led to wrongful convictions. One of the most high profile cases in which such a mistake was made is the case of Brandon Mayfield who was wrongly

apprehended in the Madrid train bombing incident after a latent fingerprint obtained from the bombing site was incorrectly matched with his fingerprint [6]. An extensive account of similar cases have been brought to light by Innocence project [7]. Due to these incidents and findings, the importance of latent fingerprints as forensic evidence has been undermined. This is evident from a recent ruling of a Baltimore court [8] which excluded fingerprints as evidence in a murder trial because the prosecutor was not able to justify the procedure followed for latent fingerprint matching as being sufficiently error free.

It is often argued that matching a latent fingerprint to a full-print is more of an "art" than "science" [9] because the matching is based on subjective appraisal of the two fingerprints in question by a human examiner. Moreover, the decisions made by latent examiners are required to be "crisp", i.e., an examiner can provide only one of the three decisions, viz., individualization (identification or match), exclusion (non-match) and inconclusive [4], [5]. Often latent examiners have a huge backlog of cases and are usually under time pressure to evaluate a fingerprint pair, particularly in high profile cases. Therefore, it is very important that the cases sent to latent examiners be efficiently selected and prioritized so that he/she can spend adequate amount of time in matching them. One way to achieve this goal is to design an efficient and highly accurate automatic latent to full-print matching system which should be able to provide a quantitative estimate of the probability that two fingerprints being compared belong to same finger.

In order to deal with efficiency, the concept of "Lights-Out System" for fingerprint matching has been introduced [2]. A "Lights-Out System" for fingerprint identification is characterized by no human intervention throughout the whole identification process. Such a system should automatically extract features from fingerprints and match them with a gallery database to obtain a set of possible "hits" with high confidence so that no human intervention is required. However, in latent matching only "Semi Lights-Out Systems" are feasible due to the limitations of existing technology. In a "Semi-Lights-Out System" some human intervention is allowed during feature extraction e.g. orienting the fingerprint, marking the region of interest, etc. A "Semi Lights-Out System" outputs a list of candidates that need to be examined by a latent examiner to accept or reject a fingerprint pair as a match.

Although tremendous progress has been made in developing automated fingerprint identification systems (AFIS), most of these systems work well only in scenarios where the matching is performed between rolled or plain fingerprint images. The results of Fingerprint Vendor Tech-

TABLE I

PERFORMANCE OF A REPRESENTATIVE LATENT MATCHER (LATENT VS. ROLLED OR LATENT VS. PLAIN) ON A DATABASE OF MORE THAN 40 MILLION SUBJECTS [2]

Quality of Latents	Type of Mate		
	Latent vs. Rolled	Latent vs. Plain	Latent vs. Mixed Rolled/Plain
Good and Better	94%	63%	78%
Average Case Work	54%	39%	47%

nology Evaluation (FpVTE) conducted by NIST [10] show that the most accurate commercial fingerprint matchers can achieve a rank-one identification rate of more than 99.4% on a database of $10,000$ plain fingerprint images (see results of Medium Scale Test on page 56 in [10]). On the other hand, the accuracy of latent to full print match continues to be quite low. The NIST latent fingerprint testing workshop reports that the rank-one accuracy of an automatic latent matcher can be as low as 54% on a large database of more than 40 million subjects [2] (see Table I).

AFIS systems have not been very effective so far in matching latent fingerprints because the challenges involved in latent print matching are quite different from full (rolled or plain) fingerprint matching. The difficulty in latent matching is due to three main reasons: (i) poor quality of latent prints in terms of the clarity of ridge information, (ii) latent print area can be quite small compared to the full print and (iii) large non-linear distortion due to pressure variations. Figure 2 shows a sample latent image from the NIST Special Database-27 along with its corresponding full print image. In Figure 2(a), the ridge information in the middle of the image is obscured by the presence of background noise, extraneous markings and other spurious friction ridges surrounding it. Further, while a typical rolled fingerprint has more than 60 minutiae, a typical latent fingerprint may have only 15 usable minutiae [2]. Thus, latent fingerprint identification is a difficult problem which needs immediate attention.

The latent identification process can be divided into four steps, namely, (i) Analysis, (ii) Comparison, (iii) Evaluation and (iv) Verification. This process is commonly referred to as the ACE-V procedure in latent fingerprint literature [11].

- Analysis refers to assessing the latent fingerprint to determine whether sufficient ridge information is present in the image to be processed and to mark the features along with the

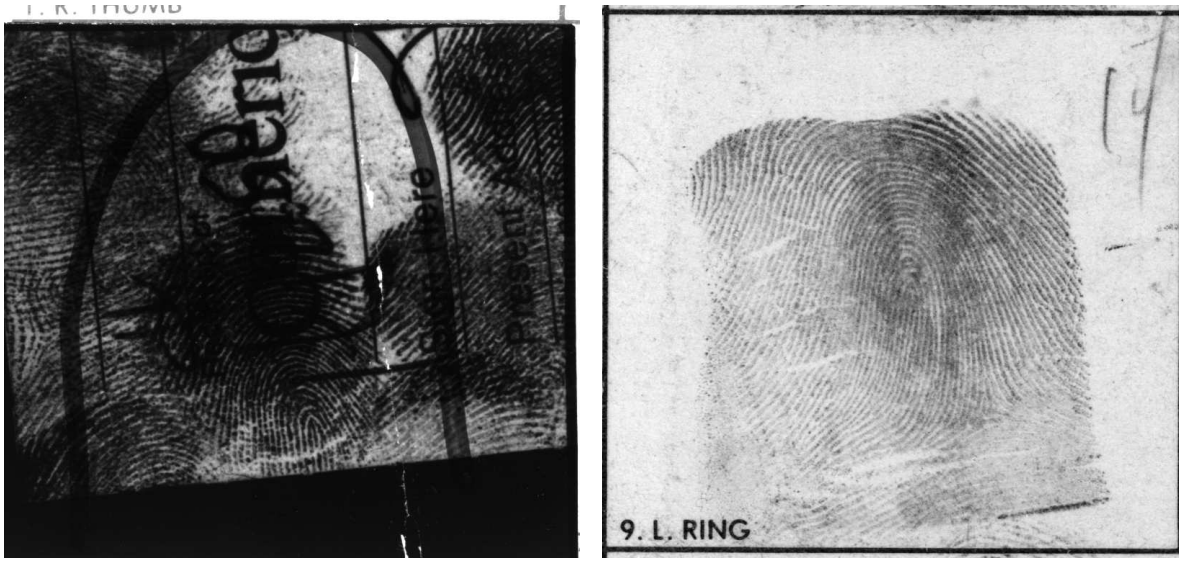

(a) (b)

Fig. 2. A sample fingerprint pair from the NIST Special Database-27. (a) Latent print, (b) full print.

associated quality information. The latent print analysis is usually performed manually by a human expert in total objectivity (without having access to a reference print). Features in a fingerprint can be divided into three levels. Level 1 features usually refer to features based on global pattern of the fingerprint. Level 2 features refer mainly to minutiae points and Level 3 features refer to the other characteristic features like ridge shape, pores, incipient ridges, creases, worts, etc. Note that level 1 features are not very informative for matching and are typically used for fingerprint classification which can facilitate exclusion of full prints whose patterns do not match with the query latent print. Level 2 features however are considered the most informative features in a fingerprint.

- Comparison refers to the stage where an examiner compares a latent image to a reference print to ascertain their similarities or dissimilarities. Features at all three levels are compared at this stage.
- Evaluation stage refers to classifying the fingerprint pairs as individualization (identification or match), exclusion (non-match) or inconclusive.
- Verification is the process of re-examination of a fingerprint pair independently by another examiner in order to verify the results of the first examiner.

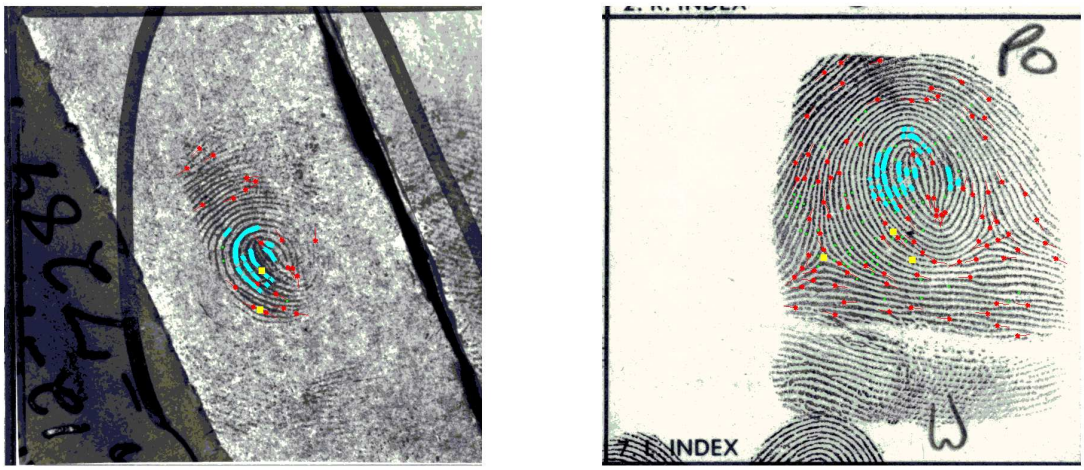

(a) (b)

Fig. 3. A sample fingerprint pair from the NIST Special Database-27 with minutiae, incipient ridges, dots and pores marked. (a) Latent print with manually marked features, (b) full print with automatically extracted minutiae. Pores are shown as small dots, incipients are shown as thick cyan lines, dots are shown as yellow squares and minutiae are marked with stars with tail oriented along minutia direction.

In this study, we assume that the analysis of the latent print has been performed manually by a latent examiner who has marked the minutiae details, the ridge flow information and other level 3 features such as incipient ridges. We focus mainly on the comparison stage where the manually marked features in the latent are matched against the features extracted automatically from the full-print images (see figure 3). Our contributions are three-fold: (i) we present a minutiae-based matcher that takes into account the specific characteristics of matching a latent with its corresponding full-print; (ii) we develop a ridge-correlation based matcher to ascertain the similarity in the ridge structure between the latent and full-print images; (iii) we perform a fusion of the minutiae and ridge-correlation matchers to improve the overall matching accuracy.

II. Minutiae-based Matching

Minutiae-based matching is an important part of the overall matching procedure proposed in this study. Matching latent fingerprints with full-prints is quite different in certain aspects and in fact more difficult than matching a rolled or flat print with a print obtained in a similar manner. We therefore make the following assumptions that are reasonable while matching a latent with

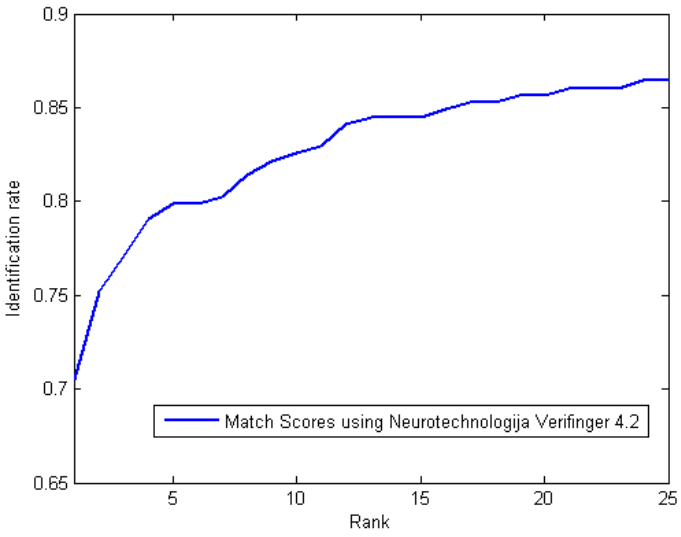

Fig. 4. Cumulative Match Characteristic (CMC) curve corresponding to matching manually marked latent minutiae with manually marked full-print minutiae using Neutechnologija Verifinger 4.2.

a full-print.

1) The latent print is fully contained in its corresponding full-print.
2) Given that the minutiae in latent are marked by a latent examiner, there is little chance of a spurious minutia being present in the latent.
3) Full-print is typically of good quality and hence the chances of missing a minutiae in the full-print is negligible.

Based on the above assumptions, when latent print is matched against its corresponding full-print, all the latent minutiae are expected to have a match in the full-print while the converse need not be true.

Commercial minutiae-based matchers are typically designed for full-print to full-print matching and do not take into account the specific characteristics of latent to full-print matching. Hence, they fail to perform well for the task of latent minutiae matching. For example, the COTS matcher in [12] has a rank-one accuracy of 95% on the Medium Scale Test in FpVTE [10]. However, the same matcher has a rank-one accuracy of about 70% when matching latent minutiae to full-print minutiae in the NIST-SD27 database (see Figure 4).

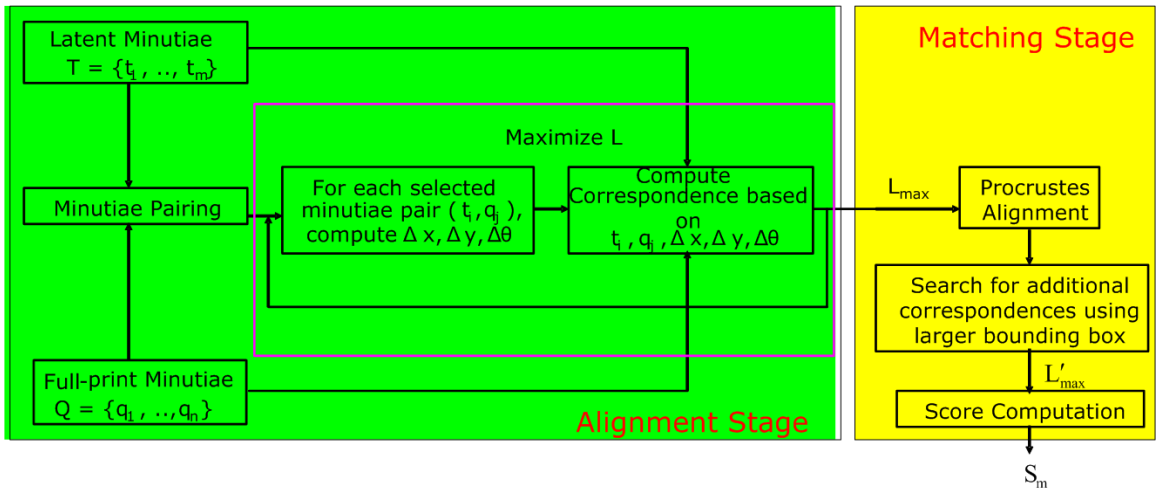

Fig. 5. Schematic diagram of the proposed minutiae-based matcher for matching latent images to full-print images.

The specific nature of latent to full-print matching requires a fingerprint matcher designed exclusively for this purpose. The schematic diagram of the proposed minutiae-based matcher is shown in Figure 5. Due to the poor quality of latent fingerprints, minutiae location and direction are noisy even though they are manually marked by a latent examiner. In addition, the relative deformation present between two fingerprints being compared makes minutiae matching more difficult. Therefore, we detect the minutiae correspondences in two stages. In the first stage we obtain the initial minutiae correspondences as follows. Let $T = \{t_1, t_2, \cdots, t_m\}$ be the set of m minutiae in the latent image, where $t_i = (x_i^t, y_i^t, \theta_i^t), i = 1, 2, \cdots, m$ represents the location (x_i^t, y_i^t) and direction (θ_i^t) of the i^{th} minutia point. Let $Q = \{q_1, q_2, \cdots, q_n\}$ be the set of n minutiae in the full-print, where $q_j = (x_j^q, y_j^q, \theta_j^q), j = 1, 2, \cdots, n$. For every possible minutiae pairing $(t_i, q_j), i = 1, 2, \cdots, m$ and $j = 1, 2, \cdots, n$, we compute the relative translation $(\Delta x_{ij}, \Delta y_{ij})$ and rotation $(\Delta\theta_{ij})$ between the two minutiae. If the absolute value of the rotation parameter $(|\Delta\theta_{ij}|)$ is greater than a threshold (say 45 degree), the minutiae pair is rejected. Otherwise, using these alignment parameters all the other minutiae in the full-print image are aligned with respect to the latent minutiae. After alignment, the minutiae are converted into polar coordinates with the matching pair as the center as follows

$$\begin{pmatrix} r_j^q \\ e_j^q \\ \gamma_j^q \end{pmatrix} = \begin{pmatrix} \sqrt{(x_j^q - x_*^t)^2 + (y_j^q - y_*^t)^2} \\ tan^{-1}(\frac{y_j^q - y_*^t}{x_j^q - x_*^t}) \\ \theta_j^q - \theta_*^t \end{pmatrix}, \quad (1)$$

where $(x_j^q, y_j^q, \theta_j^q), j = 1, 2, \cdots, n$ are the coordinates of the full-print minutia after alignment, $(x_*^t, y_*^t, \theta_*^t)$ are the coordinates for the reference (matching) latent minutia and $(r_j^q, e_j^q, \gamma_j^q)$ are the coordinates of the full-print minutiae in the polar coordinate system. Note that r represents the radial distance, e represents the angle that the line joining the minutia and the center makes with x-axis and γ represents the relative direction of the minutia with respect to the reference minutia. Similarly, the latent minutiae are also expressed in the polar coordinate system as $\{(r_i^t, e_i^t, \gamma_i^t), i = 1, 2, \cdots, m\}$. While the representation of minutiae in the the polar coordinate system is similar to the representation used in [13], our matching procedure is different from the one described in [13].

For each latent minutia (say $(r_i^t, e_i^t, \gamma_i^t)$), we obtain a list of prospective full-print minutiae matches by finding the full-print minutiae (say $(r_j^q, e_j^q, \gamma_j^q)$) lying in its neighborhood such that

$$\Psi(e_j^q, e_i^t) < \epsilon_e^j, \quad (2)$$

where $\Psi(\theta_1, \theta_2) = min(|\theta_1 - \theta_2|, 360 - |\theta_1 - \theta_2|)$ is the angular difference function, $\epsilon_e^j = tan^{-1}(\frac{\epsilon_e}{r_j^q})$ and ϵ_e is a constant threshold. The prospective matches are sorted according to radial angle e and list is searched for the first minutia $(r_j^q, e_j^q, \gamma_j^q)$ that satisfies the following conditions:

$$|r_j^q - r_i^t| < \epsilon_r, \quad (3)$$

$$\Psi(\gamma_j^q, \gamma_i^t) < \epsilon_\gamma, \quad (4)$$

where ϵ_r, and ϵ_γ are constant thresholds. The minutia that satisfied Eqns 2, 3 and 4 is assigned as the corresponding minutia for the latent minutia $(r_i^t, e_i^t, \gamma_i^t)$. We thus obtain the set of correspondences for the latent minutiae based on the alignment generated by every minutiae pair. We retain only the set of correspondences that produces the maximum number of matching minutiae (say L).

Due to the large relative deformation between the latent and full-print images, the matching scheme described earlier may not identify all the true minutiae correspondences between the

latent and the full-print. We overcome the problem due to deformation in the following manner. Based on all the matching minutia pairs identified in the previous step, we compute a new set of alignment parameters using the Procrustes algorithm [14]. The new alignment parameters are more robust because they are computed using all the matching minutiae. The full-print minutiae are aligned with the latent minutiae and the known correspondences in the two minutiae sets are removed. For each latent minutia (say (x^t, y^t, θ^t)) for which a corresponding full-print minutia has not been identified, we verify whether there exists a full-print minutia (say (x^q, y^q, θ^q)) such that

$$\sqrt{(x^q - x^t)^2 + (y^q - y^t)^2} + w_\theta * (\Psi(\theta^q, \theta^t)) < \epsilon_s, \tag{5}$$

where w_θ is the weight assigned to the angular difference and ϵ_s is a constant threshold. If such a full-print minutiae can be found, we consider it as an additional correspondence. Let the number of additional correspondences obtained using this larger bounding box be L_{new}. Since these additional correspondences are less reliable than the initial correspondences, we assign a smaller weight to the additional correspondences and compute the weighted correspondence score $L^{'}$ as

$$L^{'} = L + w_1 * L_{new}, \tag{6}$$

where $w_1 < 1$.

A number of match score functions have been proposed to compute the similarity between two fingerprints. For example, Jain et al. [13] proposed the function in equation (7) that normalizes the number of matched minutiae pairs based on the number of minutiae in the template and query prints. If L is the number of matching minutiae pairs and m and n are the number of minutiae in the query and template prints, respectively, then the match score S_m can be computed as,

$$S_m = 100 \frac{L}{max(m, n)}. \tag{7}$$

The score function in equation (7) does not account for the fact that there may be only a partial overlap between the two prints being matched in which case the score will be undesirably low even if the overlapping area is perfectly matching. A modified score function was proposed in Jain et al. [15] to account for these limitations. If m_o and n_o are the number of minutiae in

the overlapping regions of the query and template prints, respectively after alignment, then the match score S_m is computed as

$$S_m = L \times \frac{L - w_2 * (m_o - L)}{m_o + 1} \times \frac{L - w_2 * (n_o - L)}{n_o + 1}, \tag{8}$$

where w_2 is the weight used to penalize non-matching minutiae (set to 0.2 in [15]). The score function in equation (8) is also not well-suited for matching latents with full-prints due to two reasons. Since the number of matching minutiae can be quite small (an average of 15 in NIST SD-27) in latent to full-print matching, the first product term (L) in equation (8) makes the score highly dependent on just the number of matches. Secondly, due to the poor quality of latent images, there may be many missing minutiae in the latent. Therefore, while latent minutiae that do not have a corresponding match in the full-print must be penalized, the full-print minutiae that do not have a match in the latent should not be penalized. Based on these considerations, we propose a new match score function which is computed as follows.

$$S_m = \frac{L^{'}}{m + 1} + \frac{L^{'}}{n_o + 1} - w * \frac{m - L^{'}}{m + 1}, \tag{9}$$

where w is the weight given to the penalty term and n_o is the number of full-print minutiae lying the overlapping segmented region after the full-print has been aligned with the latent print during the minutia matching procedure.

We can summarize the complete minutiae-based matching algorithm as follows.

1) Consider each latent - full-print minutia pair (t_i, q_j), compute the transformation parameters $(\Delta x_{ij}, \Delta y_{ij}, \Delta\theta_{ij})$.
2) Transform all the full-print minutiae according to $(\Delta x_{ij}, \Delta y_{ij}, \Delta\theta_{ij})$.
3) If $\Delta\theta_{ij} > \epsilon_\theta$ do not consider (t_i, q_j) as a possible correspondence for further consideration and start from step 1 with a different minutia pair (t_i, q_j).
4) Compute the correspondences between latent and full-print minutiae using equations (3) (2) and (4).
5) Follow steps (1) to (4) until all possible pairs (t_i, q_j) have been considered.
6) Find the pair (t_i, q_j) which gives the largest number of correspondences (say L). These L correspondences are retained for further processing.
7) Align the corresponding minutiae obtained in step (6) using Procrustes analysis.

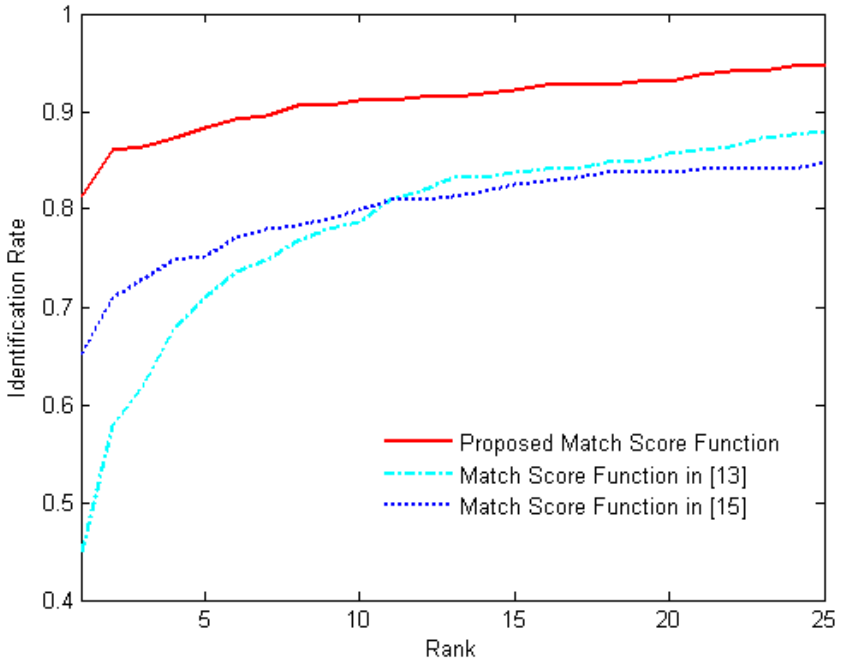

Fig. 6. CMC curves comparing the performance of different minutiae match score functions.

8) For all the non-matching latent minutiae, find their corresponding full-print minutiae using a large tolerance window as specified in equation 5.
9) Update the number of correspondences found using equation (6) with the new correspondences found in step (8) and call it $L^{'}$.
10) Compute the matching score using equation (9).

Figure 6 compares the identification results obtained using the three match score functions presented in Eqns. (7), (8) and (9). We observe that the proposed match score function in Eq. (9) significantly outperforms the other two functions.

III. Ridge Correlation

Due to inherent difficulties in minutiae-based matching such as distortion, missing minutiae etc., minutiae information alone may not be sufficient for matching latent prints. An alternate source of discriminatory information that can be used in matching is the ridge-flow pattern which is much more reliable than minutiae in the presence of noise. We shall now describe the

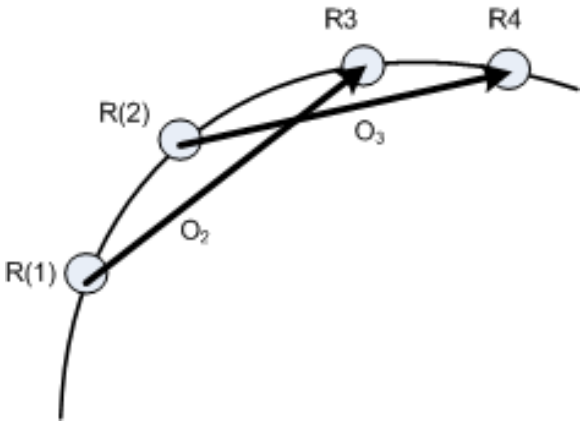

Fig. 7. Orientation vector computation at different points on a ridge.

procedure for obtaining the correlation score between the sets of ridges in latent and full-print images being matched. Let a ridge be represented as $R^k = \{R^k(i) = (x_i^k, y_i^k), i = 1, 2, \cdots, N_{R^k}\}$ where (x_i^k, y_i^k) represents the location of the i^{th} point on the k^{th} ridge and N_{R^k} is the total number of points in that ridge. At any point on a ridge, the orientation vector is defined as

$$\vec{o} = \frac{(R^k(i+\delta) - R^k(i-\delta))}{|(R^k(i+\delta) - R^k(i-\delta))|}, \tag{10}$$

where δ is set to 10 in the experiments. For computational efficiency, we sample the ridge lines at an interval of about 10 pixels and compute the orientation vectors at these points for both latent and full-print ridges. Figure 7 shows the orientation vectors computed along a ridge. Thinned ridge lines for the full-prints are obtained automatically using the algorithm described in [13] whereas the ridges for the latent images were manually marked (see Figure 8).

The ridge correlation score between latent and full-print is computed as follows. First the ridge lines are aligned using the parameters obtained from Procrustes analysis based on the minutiae correspondences as described in Section II. For each ridge point in the latent image, the nearest ridge point in the full-print image is found with the constraint that the distance between these points is no more than a specified threshold. Then, the magnitude of difference (say d_i) of the orientation vectors at these corresponding points (say q_i and t_i) is computed using the following equation:

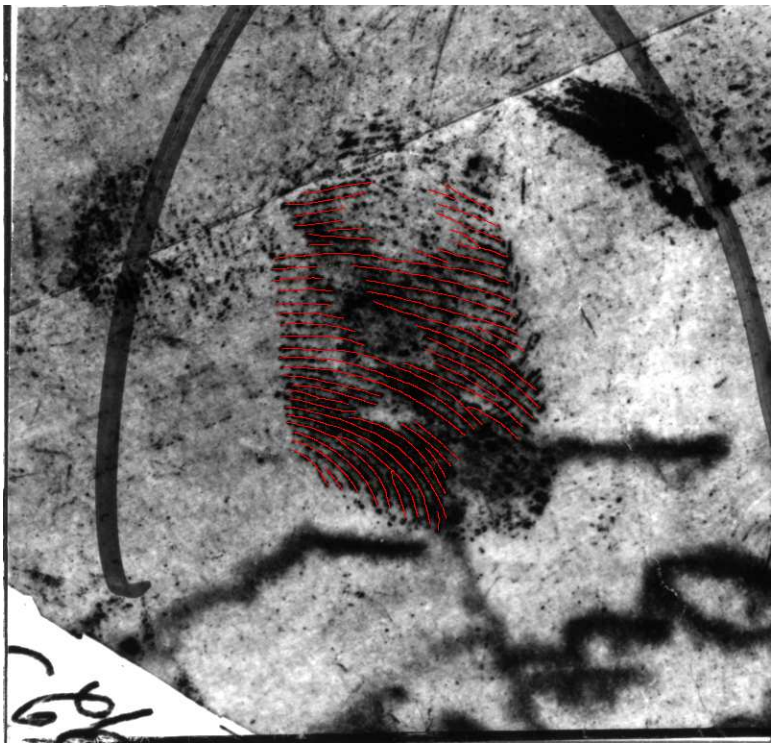

Fig. 8. A sample latent image with manually marked ridges from the NIST SD-27.

$$d_i = min(|\vec{o}_{ti} - \vec{o}_{qi}|, |\vec{o}_{ti} + \vec{o}_{qi}|), \tag{11}$$

where $\vec{o}_{ti}$ and $\vec{o}_{qi}$ are the orientation vectors at the corresponding ridge points in the latent and full-print images, respectively. The ridge correlation score between two fingerprints is defined as the average correlation score between all the ridges in the overlapping region of the two prints,

$$S_r = -\frac{1}{N_R}\sum_{i=1}^{N_R} d_i. \tag{12}$$

where N_R is the total number of ridge points in either print that has a corresponding ridge point in the other image. Note that d_i's represent difference in the two corresponding orientation vectors while S_r gives the similarity between two ridges due to the negative sign in Eq. 12.

Figure 10 shows an example of the manually extracted ridges in a latent fingerprint overlaid over the automatically extracted ridges of the corresponding full-print image. The discriminatory power of the ridge correlation matcher can be seen from the CMC curve shown in Figure 9.

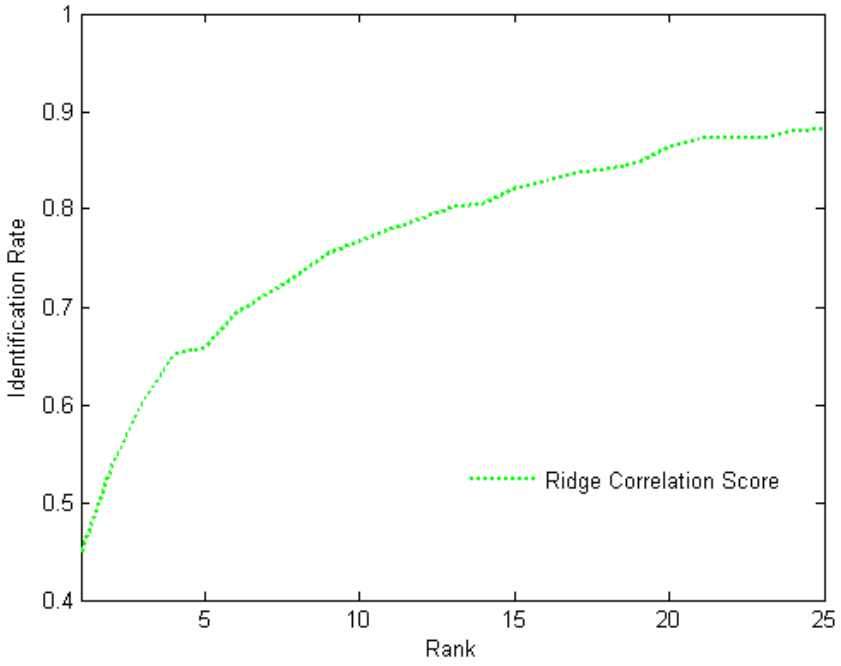

Fig. 9. CMC curve corresponding to the Ridge Correlation matcher.

While ridges are not as valuable as minutiae in terms of latent to full-print matching, the next section shows that fusion of the two match scores improves the overall accuracy.

IV. Fusion of Minutiae and Ridge Correlation Scores

In order to take advantage of both the minutiae matcher and the ridge correlation matcher, it is necessary to combine the scores to compute a new score which best discriminates the correct and incorrect latent full-print matches. We use the min-max normalization technique and weighted sum of scores fusion technique to perform fusion of minutiae and ridge-correlation matchers. This particular scheme for fusion is chosen since it is more resilient to noise in either of the two scores [16]. The min-max normalization is applied separately for each latent matching as follows.

$$SNorm_{min_{ij}} = \frac{S_{min_{ij}} - min(S_{min_i})}{max(S_{min_i}) - min(S_{min_i})}, \tag{13}$$

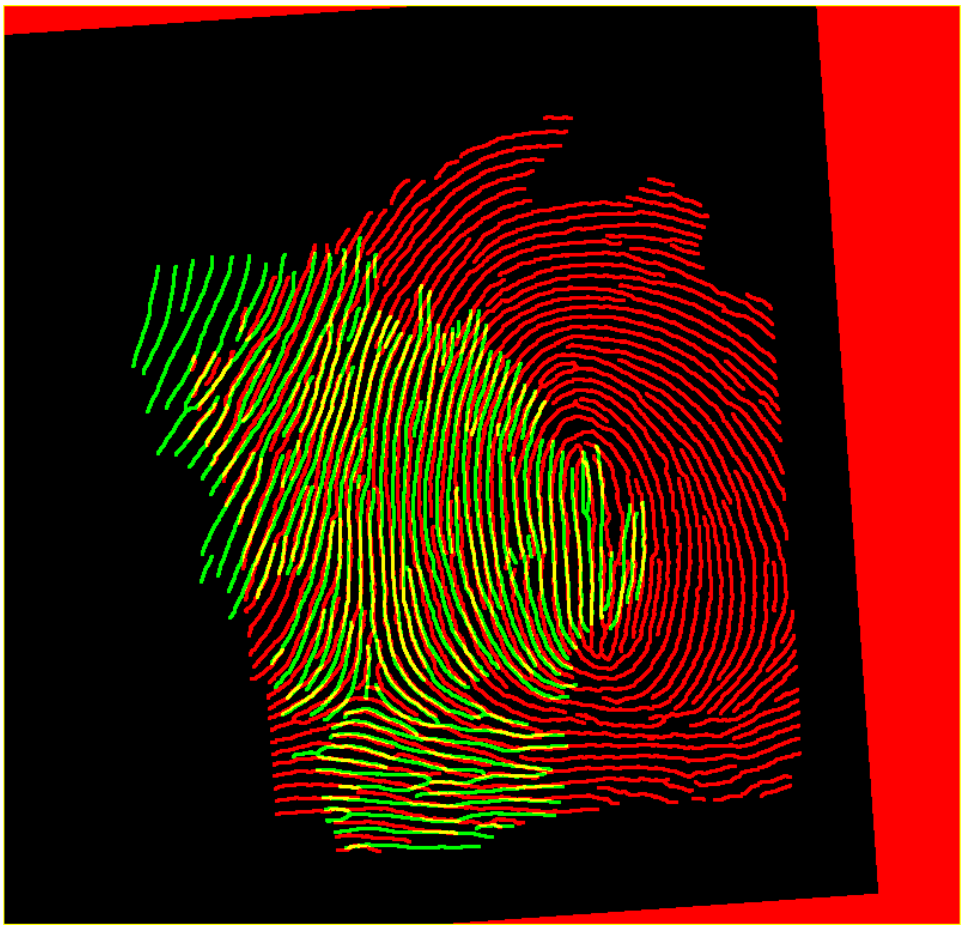

Fig. 10. Manually extracted ridges of latent fingerprint overlaid on the automatically extracted ridges in the corresponding full-print image.

where $S_{min_{ij}}$ corresponds to minutiae score obtained by matching i^{th} latent with j^{th} full-print image and S_{min_i} corresponds to the set of scores obtained by matching i^{th} latent with all the full-print images. The ridge correlation scores are also normalized using the same procedure. The fusion score is obtained as

$$SFusion_{ij} = \alpha_{min} * SNorm_{min_{ij}} + \alpha_{rid} * SNorm_{rid_{ij}}, \tag{14}$$

where $SNorm_{rid_{ij}}$ is the normalized ridge correlation score and α_{min} (say 0.4) and α_{rid} (say 0.6) are weights given to minutiae and ridges matching scores.

Figure 11 shows an example of a genuine pair where the fusion of ridge correlation score with

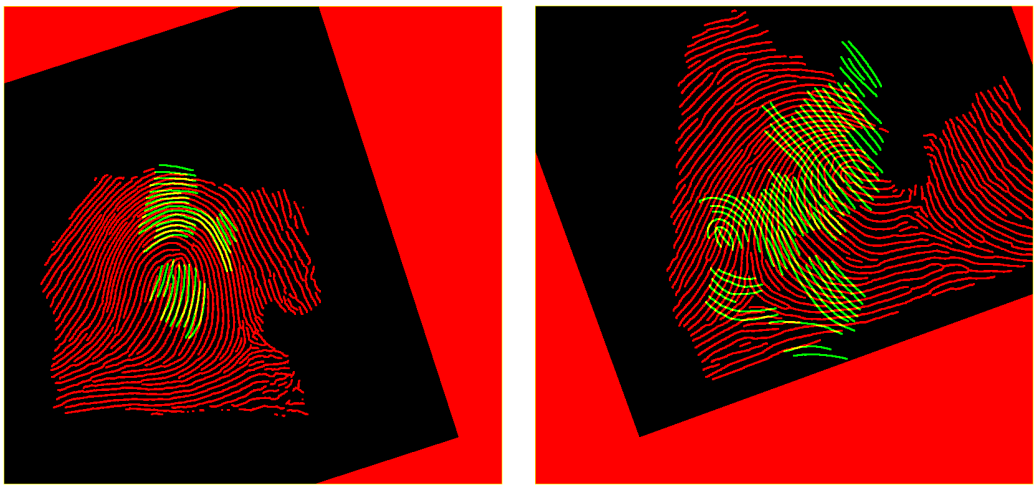

(a) (b)

Fig. 11. Manually extracted ridges of latent fingerprint overlaid on automatically extracted ridges of the corresponding full-print image for case where (a) fusion score improves the rank and (b) where fusion score degrades the rank of a genuine pair.

the minutiae matching score improves the rank of the retrieved genuine full-print and another example where it degrades the rank. It is clear that the decrease in rank in the second case is due to the incorrect alignment obtained from the minutiae matcher.

V. EXPERIMENTS AND RESULTS

The experiments were conducted on NIST Special Database-27 [2] which contains 258 latent fingerprints and their corresponding full-print images. These 258 latent prints are divided into three classes namely: Good, Bad and Ugly based on the quality of latent fingerprints (see Figure 12) in the database. There are 88 “Good”, 85 “Bad” and 85 “Ugly” latent images in the database. Since two latent images in the database had the same corresponding full-print, each latent is compared with only 257 full-print images in all the experiments.

Since latent prints are usually lifted from a complex background, it is very difficult to design an automatic segmentation algorithm to extract the region of interest. We therefore manually segment the latent images while taking care that the region of interest contains the least amount of background region. Further, since the latent fingerprints are not of good quality, ridges are manually marked on the latent images. A sample of latent fingerprint with manually marked ridges is shown in Figure 8.

(a) (b) (c)

Fig. 12. Examples of latent images in the NIST Special Database-27 from (a) "Good" category, (b) "Bad" category, and (c) "Ugly" category.

For the latent fingerprints in NIST SD-27 database, we used the ground truth minutiae supplied with the database for our experiments as any automatic minutiae extraction algorithm is likely to fail due to poor quality. For full fingerprint images we experimented with both the automatically extracted minutiae as well as the ground truth minutiae supplied with the database. Since there are some irrelevant markings present in the full-print images, manual segmentation was done on the full-print images to obtain a mask for the region of interest. Only the minutiae falling inside the region of interest were considered for processing. Figure 13 shows an example of the masks obtained for a latent as well as a full-print image. Figure 14 shows examples of latent and full-print images with minutiae marked. It was observed that even in full-print images, automatic minutiae extraction algorithm does not perform well in some cases.

Figure 15 shows the CMC curves corresponding to the ridge correlation score, minutiae matching score as well as the fusion of these two scores for both ground truth full-print minutiae as well as automatically extracted full-print minutiae. It can be seen that the fusion of ridge correlation scores and the minutiae matching scores improves the performance to around 92% retrieval at rank 25 where the performance of the minutiae based matcher is around 88% and that for ridge correlation is around 86% for the case where full-print minutiae are automatically extracted. In the case where ground truth minutiae were used for full-print images, the performance of the fused system improves to around 98% retrieval at rank 25, from 95% for minutiae based matcher and 88% for ridge correlation matcher. Note that since the alignment of

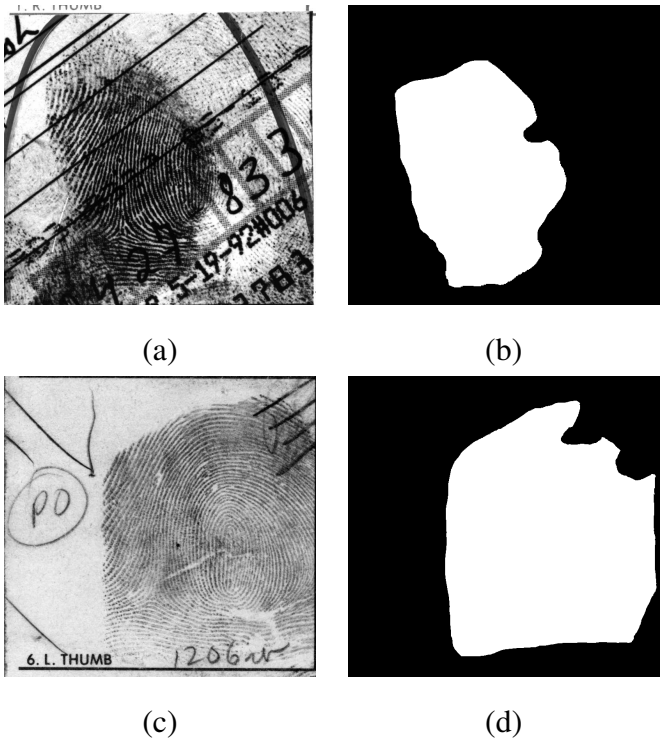

Fig. 13. Sample latent and full-print images with masks obtained by manual segmentation.

ridges were done using the parameters obtained from the minutiae matcher, there is difference between the ridge correlation scores corresponding to automatically extracted and ground truth full-print minutiae. We observe that even with correct manual segmentation, the performance drops by around 5% at rank 25 when automatically extracted minutiae are used. This indicates there is a large scope of improvement in the current minutiae extraction algorithms. Figure 16 shows the results individually for good, bad and ugly quality latent prints.

VI. Summary and Future Work

We have developed a system for matching latent fingerprints with full-prints. Due to the specific characteristics of the latent to full-print matching problem, commercial-off-the-shelf matchers that are generally designed for full print to full print matching do not perform well in the latent matching scenario. We propose a minutiae matching algorithm that is specifically designed for matching latent with full-print images. Further, we have shown that ridge correlation scores can be combined with minutiae matching scores to improve the accuracy of the system. Experiments

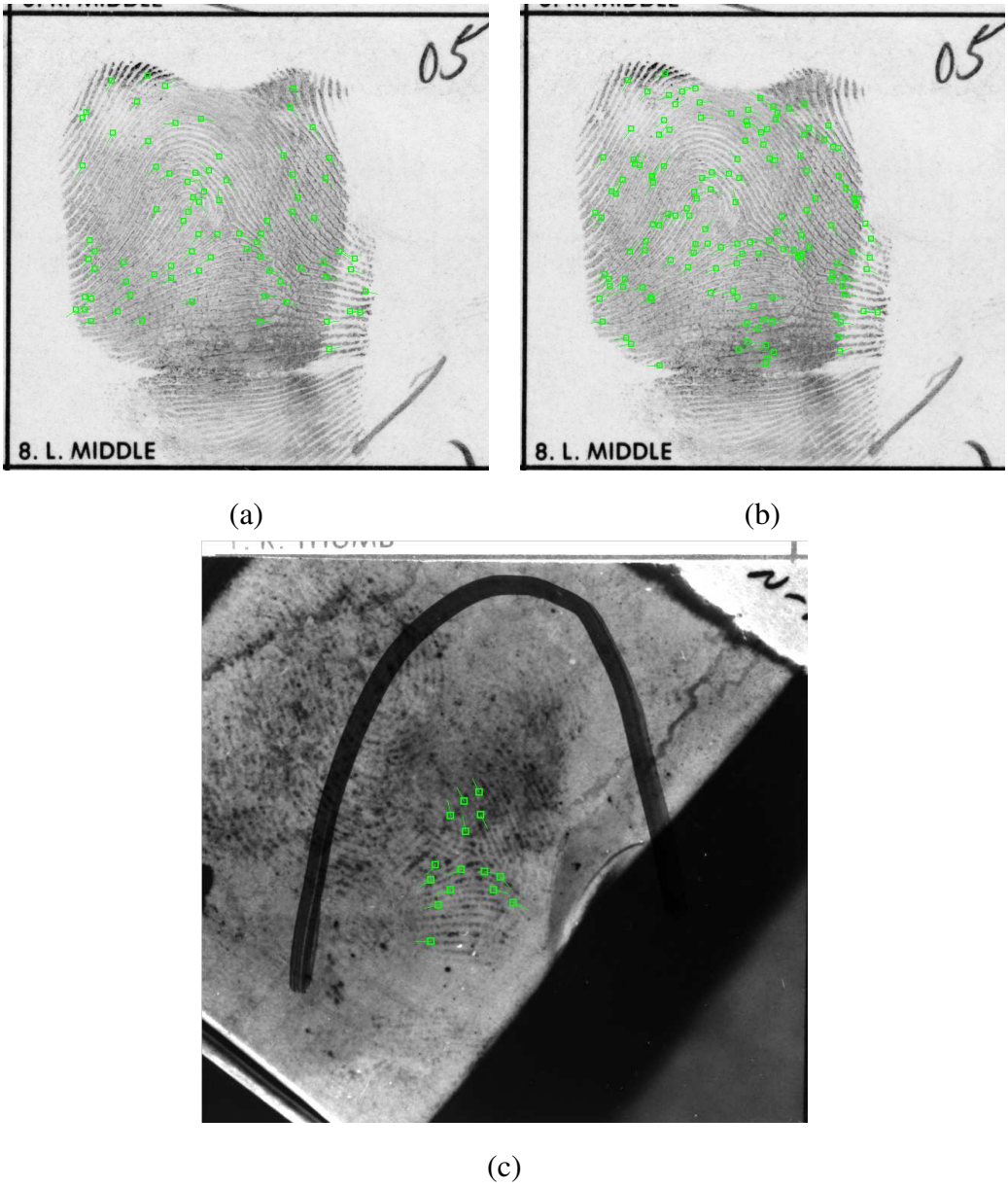

Fig. 14. Sample images from NIST SD-27 with minutiae overlaid. (a) a rolled image with ground truth minutiae overlaid, (b) the same image as in (a) with minutiae extracted using Neurotechnologija VeriFinger 4.2 [12] and (c) shows the corresponding latent image with minutiae overlaid.

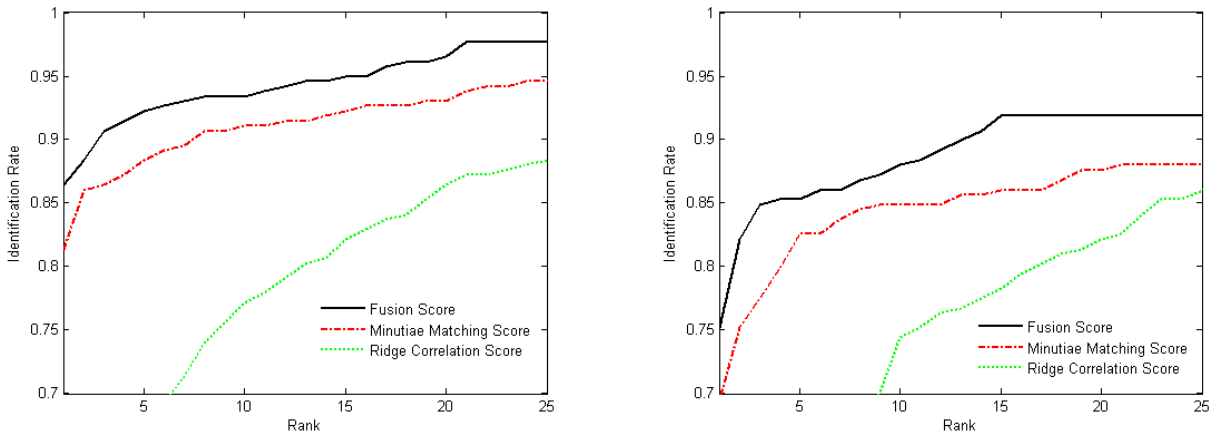

Fig. 15. CMC curves corresponding to the ridge correlation score, minutiae matching score and the fusion score for case (a) when ground truth full-print minutiae are used, (b) when the minutiae in full-print are automatically extracted using Neurotechnologija VeriFinger 4.2.

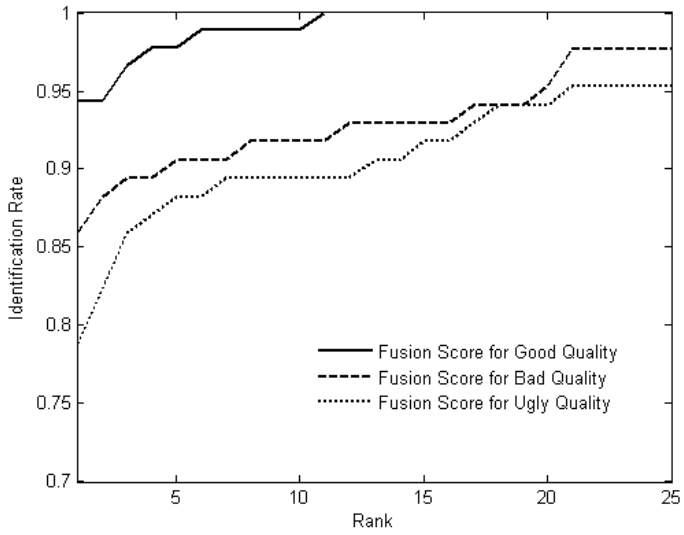

Fig. 16. CMC curves corresponding to fusion scores of Good, Bad and Ugly quality latent images in NIST SD-27 database. Each category contains 88, 85 and 85 latent images respectively.

conducted on the NIST Special Database-27 which contains 258 latent and their corresponding full-print images, shows that the proposed matcher achieves better performance compared to a commercial-off-the-shelf matcher which is known to perform quite well on full print images.

As future work, level-3 features, e.g. incipient ridges, dots and pores, will be incorporated during latent matching to improve the performance. It is expected that in case of a genuine latent full-print pair, the level-3 features will also overlap when the two images are aligned using minutiae thereby providing additional evidence for match. Note that encoding the level-3 features as additional minutiae points augmenting the available minutiae set will not be of much help. This is because there are very few level-3 features visible in latent images while in full-print images their number is very high leading to greater chances of random correspondence in non-mate pairs. Another important aspect of latent fingerprint matching is enhancement of latent fingerprints which would help avail the discriminative information available in texture of latent images. Due to bad quality of latent images, it would be fruitful to incorporate the manually marked ridges in the enhancement routine to obtain a reliably enhanced print.

REFERENCES

[1] D. Maltoni, D. Maio, A. K. Jain, and S. Prabhakar, *Handbook of Fingerprint Recognition*. Springer-Verlag, 2003.

[2] V. N. Dvornychenko and M. D. Garris, "Summary of NIST latent fingerprint testing workshop," NISTIR 7377, November 2006, http://fingerprint.nist.gov/latent/ir_7377.pdf.

[3] P. Komarinski, Ed., *Automated Fingerprint Identification Systems (AFIS)*. Elsevier Academic Press, 2001.

[4] H. C. Lee and R. E. Gaensslen, Eds., *Advances in Fingerprint Technology*. New York: CRC Press, 2001.

[5] P. M. Christophe Champod, Chris Lennard and M. Stoilovic, Eds., *Fingerprints and Other ridge Skin Impressions*. CRC Press, 2004.

[6] "A review of the FBI's Handling of the Brandon Mayfield Case," Office of the Inspector General, Special Report, March 2006, http://www.usdoj.gov/oig/special/s0601/PDF_list.htm.

[7] Case Profile, Innocence Project, http://www.innocenceproject.org/Content/73.php.

[8] "Conclusion of circuit court judge susan souder - grants motion to exclude testimony of forensic fingerprint examiner - capital murder case: State of maryland v. bryan rose," October 2007, http://www.clpex.com/Information/STATEOFMARYLANDvBryanRose.doc.

[9] A. A. Moenssens, "Is fingerprint identification a science?" Forensic-Evidence.com, 1999, available at http://forensic-evidence.com/site/ID/ID0000$4_2$.html.

[10] C. Wilson, "Fingerprint vendor technology evaluation 2003: Summary of results and analysis report," NISTIR 7123, June 2004, http://fpvte.nist.gov/report/ir_7123_analysis.pdf.

[11] D. Ashbaugh, *Quantitative-Qualitative Friction Ridge Analysis: Introduction to Basic Ridgeology*. CRC Press, 1999.

[12] Neurotechnologia Inc., Verifinger, http://www.neurotechnologija.com.

[13] A. K. Jain, L. Hong, and R. Bolle, "On-line fingerprint verification," *IEEE Transactions on Pattern Analysis and Machine Intelligence*, vol. 19, no. 4, pp. 302–314, 1997.

[14] I. L. Dryden and K. V. Mardia, *Statistical Shape Analysis*. John Wiley & Sons, 1998.

[15] A. K. Jain, S. Prabhakar, and S. Chen, "Combining multiple matchers for a high security fingerprint verification system," *Pattern Recognition Letters*, vol. 20, no. 11, pp. 1371–1379, 1999.

[16] A. K. Jain, K. Nandakumar, and A. Ross, "Score normalization in multimodal biometric systems," *Pattern Recognition*, vol. 38, no. 12, pp. 2270–2285, December 2005.